Prediction methodology of critical heat flux on a heater rod under inclined and rolling conditions based on bubble tracking method and continuum percolation theory

Geon-Woo Kim [a], Jae Soon Kim [a], Hyoung Kyu Cho* [b]
[a] *Korea Institute of Nuclear Safety,62 Kwahak-ro, Yuseong-gu, Daejeon 34142, Republic of Korea*
[b] *Seoul National University,1 Gwanak-ro, Gwanak-gu, Seoul 08826, Republic of Korea*
**Corresponding author: chohk@snu.ac.kr*

Keywords: critical heat flux, simulation, inclined, rolling, bubble, percolation

1. Introduction

According to previous experiments [1-3] on CHF (Critical Heat Flux) under marine conditions, it has been reported that CHF increases when heater rod was inclined compared to the vertical condition, and decreases compared to the inclination condition during rolling condition. However, the localized phenomena regarding these CHF variations have not yet been elucidated due to the experimental conditions of high temperature and high pressure which is hard to visualize or measure the local parameters.

Meanwhile, according to recent studies [4-9] on CHF experiment, investigations were conducted on the mechanism of CHF by tracking dry patches on a boiling surface. A common conclusion from their research is that CHF is influenced significantly by the behavior of bubbles near the wall, leading to dry patch formation. In particular, some researchers [7-9] have experimentally validated that using the probability distribution of bubble presence and the size distribution of bubble near the heated wall surface, one can predict CHF in both pool boiling and flow boiling based on the continuum penetration theory [10]. This suggests that for CHF under marine conditions, if the behavior of bubbles near the heated wall under inclination and rolling conditions can be simulated or measured, CHF can be predicted using the continuum penetration theory.

There are various methods for analyzing bubble behavior near the heated wall. Among them, CFD (Computational Fluid Dynamics) analysis can provide localized information but demands significant computing power. Meanwhile, in recent research, Kim and Cho [11] proposed a methodology for modeling and tracking bubbles at the heated wall for an outside of horizontal tube to predict boiling heat transfer coefficients. According to this study, the bubble tracking method effectively predicted the heat transfer coefficient of the horizontal tube by numerically modeling bubble generation, growth, coalescence, and departure. Therefore, in this study, we applied this bubble tracking methodology to the rod shape and performed analysis for vertical, inclination, and rolling conditions to obtain bubble information near the heated wall and utilize it for CHF prediction.

In this study, preliminary calculations were conducted to predict CHF by incorporating data based on the bubble tracking model into the CHF prediction methodology of continuum penetration theory. The results of the calculations showed that this methodology predicted the trends observed in previous inclination/rolling experiments [1] well.

2. Simulation methods and results

This section briefly introduced methodologies for analyzing bubble behavior near the heated surface, detailed backgrounds of continuum percolation theory, stochastic modeling approaches for dry patch formation, and methods and results of CHF determination and calculation. The detailed theoretical frameworks, experimental data, and validation procedures for each modeling approach are elucidated in the cited references.

2.1 Bubble tracking method

The bubble tracking model utilized in this research is based on the framework proposed by Kim and Cho [11]. However, their initial model was constrained to analyzing bubbles on a stationary horizontal tube. Thus, this study outlines the adaptations made to the model to facilitate analysis under rod-shaped heating elements and conditions involving inclination and rolling. Since the existing code was only capable of analyzing the external flow of horizontal tubes, adjustments were made to account for the buoyancy direction based on the inclination angle, thereby extending its computational capabilities to encompass inclined and vertical rods. Furthermore, an external force was incorporated for the rolling simulation. Subsequently, the following force balance model for bubble tracking method was formulated.

$$\boldsymbol{\rho_v V_b a_{(\theta,z)}} = \boldsymbol{F_{tot(\theta,z)}} = \boldsymbol{F_{b(\theta,z)}} + \boldsymbol{F_{qs(\theta,z)}} + \boldsymbol{F_{s(\theta,z)}} + \boldsymbol{F_{am(\theta,z)}} + \boldsymbol{F_{add}} \quad (1)$$

$$\boldsymbol{F_{b\theta}} = (\rho_l - \rho_v) g V_b sin\theta cos\varphi \quad (2)$$

$$\boldsymbol{F_{bz}} = (\rho_l - \rho_v) g V_b sin\varphi \quad (3)$$

$$\boldsymbol{F_{qs(\theta,z)}} = -\frac{1}{2} C_D \rho_l (U_b - U_l)|(U_b - U_l)|A \quad (4)$$

$$\boldsymbol{F_{s(\theta,z)}} \sim d_w \sigma \frac{\pi(\alpha-\beta)}{\pi^2-(\alpha-\beta)^2}(sin\alpha + sin\beta) \quad (5)$$

$$\boldsymbol{F_{am(\theta,z)}} = -\frac{1}{2} V_b \rho_l a_{(\theta,z)} - 2A\rho_l (U_b - U_l)\dot{r_b} \quad (6)$$

$$\boldsymbol{F_{add}} = (\rho_l - \rho_v) V_b a_{add} \quad (7)$$

where forces for $\boldsymbol{F_b}$: buoyancy, $\boldsymbol{F_{qs}}$: quasi-steady drag, $\boldsymbol{F_s}$: surface tension, $\boldsymbol{F_{am}}$: added mass, and $\boldsymbol{F_{add}}$: additional forces due to rolling. Relating parameters are θ: circumferential position, φ: inclined angle, z: axial position, C_D: drag coefficient, U_b: bubble velocity, U_l: liquid bulk velocity, A: projected area of bubble, d_w: contact diameter, α, β : preceding/preceded contact angles, a: acceleration of bubble, r_b: bubble radius, and a_{add}: additional accelerations due to rolling.

In this code, the model presented in Table I was employed to simulate bubble departure, growth, and lift-off. It was developed to replicate water-equivalent conditions similar to the experimental setup described by Kim et al. [1,2]. However, there have been few validation studies conducted on the bubble sub-models under high-pressure conditions, resulting in a limited selection of reliable models. Despite this constraint, certain sub-models listed in Table I were utilized for Departure from Nucleate Boiling (DNB) analysis based on recent studies, encompassing nucleation site density, bubble frequency, and departure diameter. Nonetheless, there were scarce models available for inclined and rolling conditions; therefore, a qualitative investigation was conducted to elucidate bubble behavior in Ref. [3].

Table I: Bubble sub-models and assumptions for bubble tracking method

Sub-models	In this simulation
Nucleation site density	Modified Li model [12]
Bubble growth	Yoo et al. [13]
Bubble frequency	Cole [14]
Departure diameter	Kocamustafaogullari [15]
Lift-off diameter	Basu et al. [16]
Contact diameter	45% of diameter
Contact angle	α=β=41°
Bubble velocity model	Force balance model
Drag coefficient	Newton's law
Bubble shape	Spherical
Bubble interaction	Numerical
Nucleation site distribution	Random (Latin-Hypercube)

Table II: Simulation conditions of bubble tracking method

Parameters	Values
Radius of rod	9.5 mm
Heated length of rod	800 mm
Fluid	Water
Pressure	147 bar
Mass flux	300 kg/m^{2}s
Bulk fluid velocity	0.4 m/s
Bulk subcooling	2 K
Wall superheat	15 ~ 30 K
Time step	5.0 E-4 s
Calculation time	1 ~ 3 s
Inclination condition	45°
Rolling condition	45°, 6 s

Figure 1 presents a representative simulation case. When a heater rod was transitioning from a vertical (VT) to an inclination (IN) condition, bubbles are depicted to move along the heated surface in the opposite direction of gravity due to buoyancy. Under rolling conditions, tangential forces induced by acceleration from rolling result in variations in the distribution of bubbles compared to the inclination. Detailed investigations have been conducted in the previous study [3], which qualitatively affirmed the accurate modeling of bubble behavior under inclination and rolling conditions by the proposed model.

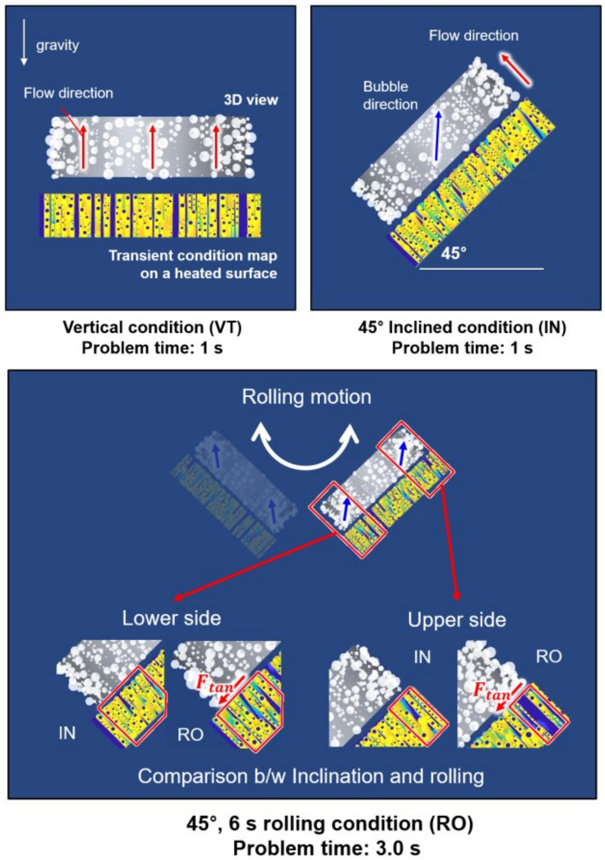

Fig. 1. Simulation results of bubble tracking method for vertical, inclined, and rolling condition (snapshot).

2.2 Background of continuum percolation theory

In previous research [4-9], thorough examination was conducted regarding the boiling process and the occurrence of boiling crisis. These studies revealed that the wetted area and the formation of dry patches play significant roles in determining CHF. Furthermore, experimental evidence suggests that boiling crisis primarily arise due to microscale interactions between the liquid and the solid surface near the heating source. Therefore, it is crucial to comprehend the behavior and interaction of bubbles near the heated surface, as well as the formation of dry patches.

Despite this challenge, recent studies on CHF modeling [7-9] have adopted a stochastic approach to accurately represent bubble interactions. This method relies on the theory of continuum percolation, a mathematical framework used to analyze critical phenomena. Continuum percolation explains how the connectivity of a system, made up of various elements, depends on the likelihood of each element's existence. Additionally, it identifies a critical probability at which an infinite number of elements become connected. This theory is widely used to understand various critical events, such as forest fires and the spread of diseases. By extending this theory beyond a grid-like structure, it becomes continuum percolation.

In the viewpoint of boiling phenomena, it can correspond to a boiling crisis. That is, it is based on the fact that a boiling crisis occurs when a large number of small bubbles are clustered together. In the context of boiling, there is a chance that bubbles will be present at each nucleation site or other positions, and these bubbles have a specific diameter at that location according to a probability distribution. As the likelihood of bubbles being present at each site increases, so does the likelihood of forming large clusters. Once a certain critical threshold is reached, a large cluster will cover most of the heating surface, signaling the onset of a boiling crisis. The following section will provide a detailed explanation of the simulation methodology.

2.3 Stochastic modeling of dry patch

This methodology was described in previous studies [7-9] and experimentally validated by applying it to pool boiling and flow boiling conditions. They calculated the probability p and radius R of bubble existence in the experiment by locations and wall superheat conditions. Using these values, Monte-Carlo simulation was performed according to the increase in heat flux, and through this, the size of the largest cluster and the second-largest cluster was obtained for each wall superheat.

This approach was outlined in prior research [7-9] and validated through experimental application in both pool boiling and flow boiling scenarios. In the experiment, the probability (p) and radius (R) of bubble occurrence were computed across various locations and wall superheat conditions. Utilizing these parameters, Monte Carlo simulation was conducted as heat flux increases. Consequently, the size of the largest and second-largest clusters was determined for each level of superheat to determine the point of boiling crisis.

What they discovered through both experimental observation and numerical analysis was a rapid decrease in the size of the second-largest cluster at the CHF. This indicates that the primary large cluster predominates on the heating surface at the critical point, with the secondary cluster failing to expand significantly even with escalating wall superheat. Ultimately, this methodology facilitates the estimation of CHF, with the key requirements being the probability of bubble formation (p) and the diameter (R) at each location across various wall superheat conditions.

In this study, the bubble tracking method is employed to estimate these two parameters, p and R. For stochastic CHF prediction, probability and radius maps are necessary for each position under vertical, inclined, and rolling conditions, as well as for each superheat condition. The simulation procedure for stochastic modeling of dry patch comprises three primary steps, as depicted in Fig. 2.

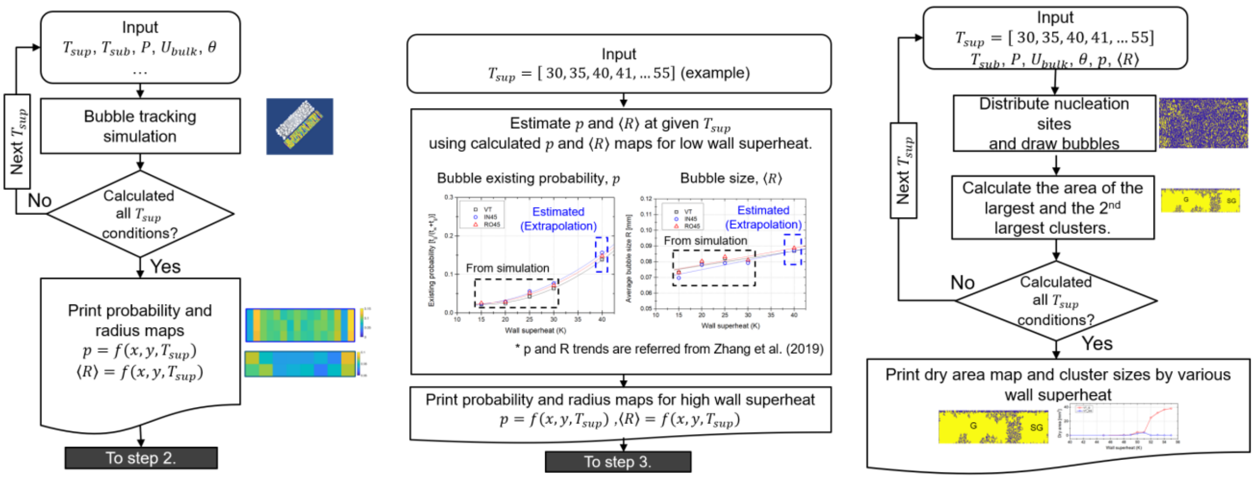

(a) Step 1: Bubble tracking method
(b) Step 2: p and R estimation for high wall superheat
(c) Step 3: Percolation simulation

Fig. 2. Simulation methodology of stochastic CHF prediction using bubble tracking method

In step 1, calculations are conducted to generate the database of p and R for each wall superheat and under vertical, inclined, and rolling conditions. Examples of these calculations are illustrated in Fig. 3. For scenarios involving high heat flux, where the number of bubbles is substantial, it is probable that the assumptions of spherical bubble shape and immediate merging—key premises underlying the bubble tracking method—may not hold true. Consequently, the analysis was restricted to superheats up to 25 K. The process of estimating p and R for high superheat conditions is elucidated in step 2.

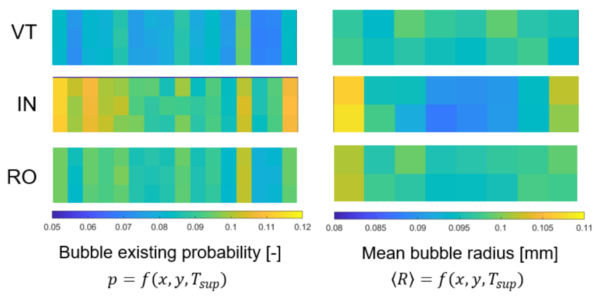

Fig. 3. Bubble existing probability (p) and mean bubble radius (R) for vertical, inclined, and rolling conditions (30 K wall superheat)

In step 2, the value at high wall superheat is estimated using the probability map and radius map derived in step 1. The estimation procedure is detailed in Ref. [7]. For the probability map, extrapolation was conducted using a quadratic function, guided by trends observed in the experimental findings [7]. Additionally, the increase in bubble size was assumed to follow a linear trend, as established in the force balance analysis of previous experiments [7]. This same approach was adopted in the current study.

In step 3, stochastic analysis is conducted. The boundary condition is the wall superheat, and when the wall superheat is specified, nucleation sites (or possible sites of bubble presence) are randomly distributed, and bubbles are generated at each site based on the provided probability and radius. Through this process, bubbles are created, and the area occupied by each bubble is determined using image processing to identify the largest and second-largest clusters (or bubbles). This process is repeated while varying the wall superheat. Calculations are carried out for predetermined superheat conditions to figure out the CHF by the variation of the size of the second-largest cluster.

2.4 Calculation of CHF

One of the results of the preliminary calculation is shown in Fig. 4. In the figure, dry patches under conditions close to CHF were plotted against wall superheat. In the accompanying graph, the sizes of the largest and second-largest clusters were shown to vary with wall superheat. The trends observed in cluster area indicated a sharp decrease in the size of the second-largest cluster. This implies that the primary large cluster prevailing at the critical point dominates the heating surface, with the secondary cluster failing to expand significantly despite the escalation in wall superheat. This point implies the boiling crisis.

The calculation results confirm the generation of a cluster under CHF conditions, and preliminary heat flux calculation was performed using the dry patch distribution and heat partitioning model. As shown in Fig. 5, it can be verified that the CHF prediction results of this study demonstrate a comparable trend to those of the previous experiment data [1] which shows the correlation between CHF values under three conditions (VT, IN, and RO).

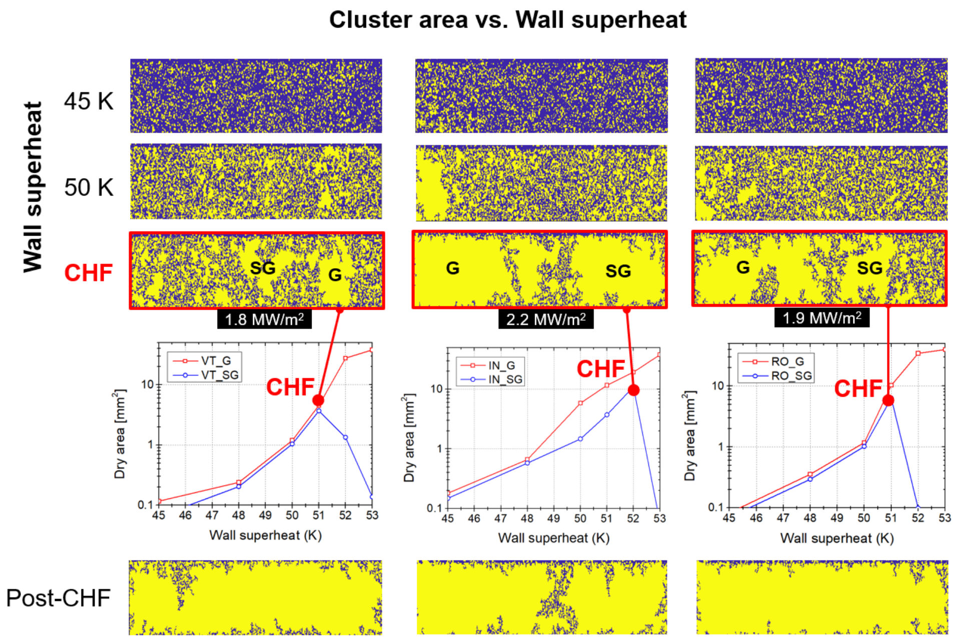

Fig. 4. Calculation example for stochastic CHF prediction

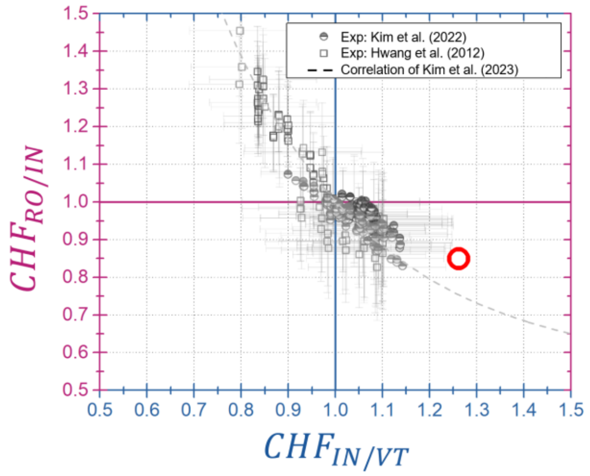

Fig. 5. Simulation result (red dot) and experimental database [9] for vertical, inclined and rolling conditions

3. Conclusions

As a result of the simulation of boiling crisis, it can be confirmed that dry patch (cluster) is generated based on the simulation result of bubble tracking method and stochastic dry patch modeling. The point of CHF can be determined by the size of the second-largest cluster, as shown in the previous studies. From the heat partitioning model, the CHF value can be calculated preliminarily. Through this analysis, it was shown that stochastic prediction of CHF is possible through mechanistic modeling of bubbles qualitatively. The result showed the similar trend of CHF for marine condition which had been experimentally investigated before. If it is based on a reliable sub-model, it is meaningful as a methodology to extend CHF prediction by analyzing the complex bubble behavior under inclined and rolling conditions.

ACKNOWLEDGEMENT

This study was supported by the Nuclear Safety Research Program through the Korea Foundation Of Nuclear Safety (KoFONS) using the financial resource granted by the Nuclear Safety and Security Commission (NSSC) of the Republic of Korea. This work does not represent the official regulatory position of KINS.

REFERENCES

[1] Kim, G. W., Yoo, J. S., Lee, C. W., Hong, H., Park, G. C., & Cho, H. K. (2022). Critical heat flux characteristics of flow boiling on a heater rod under inclined and rolling conditions. International Journal of Heat and Mass Transfer, 189, 122670.

[2] Kim, G. W., Yoo, J. S., Lee, C. W., Hong, H., Park, G. C., & Cho, H. K. (2023). Critical heat flux correlations for tube and annulus geometries under inclination and rolling conditions. Applied Thermal Engineering, 225, 120131.

[3] Kim, G. W., Experimental investigation of critical heat flux on a single heater rod under inclined and rolling conditions, Ph.D. thesis, Seoul National University, Rep. of Korea, 2021.

[4] Kim, D. E., Song, J., & Kim, H. (2016). Simultaneous observation of dynamics and thermal evolution of irreversible dry spot at critical heat flux in pool boiling. International Journal of Heat and Mass Transfer, 99, 409-424.

[5] Jung, S., & Kim, H. (2019). Observation of the mechanism triggering critical heat flux in pool boiling of saturated water under atmospheric pressure. International Journal of Heat and Mass Transfer, 128, 229-238

[6] Kim, D. E., Song, J., & Kim, H. (2016). Simultaneous observation of dynamics and thermal evolution of irreversible dry spot at critical heat flux in pool boiling. International Journal of Heat and Mass Transfer, 99, 409-424.

[7] Zhang, L. M., Seong, J. H., & Bucci, M. (2019). Percolative Scale-Free Behavior in the Boiling Crisis. Physical Review Letters, 122(13).

[8] Su, G. Y., Wang, C., Zhang, L., Seong, J. H., Kommajosyula, R., Phillips, B., & Bucci, M. (2020). Investigation of flow boiling heat transfer and boiling crisis on a rough surface using infrared thermometry. International Journal of Heat and Mass Transfer, 160, 120134.

[9] Zhang, L., Wang, C., Su, G., Kossolapov, A., Matana Aguiar, G., Seong, J. H., ... & Bucci, M. (2023). A unifying criterion of the boiling crisis. Nature Communications, 14(1), 2321.

[10] Essam, J. W. (1980). Percolation theory. Reports on progress in physics, 43(7), 833.

[11] Kim, J. S., & Cho, H. K. (2021). Advanced boiling heat transfer model for a horizontal tube with numerical analysis of bubble behaviours. International Journal of Heat and Mass Transfer, 175, 121168.

[12] Li, Q., Jiao, Y. J., Avramova, M., Chen, P., Yu, J. C., Chen, J., & Hou, J. (2018). Development, verification and application of a new model for active nucleation site density in boiling systems. Nuclear Engineering and Design, 328, 1-9.

[13] Yoo, J., Estrada-Perez, C. E., & Hassan, Y. A. (2018). Development of a mechanistic model for sliding bubbles growth prediction in subcooled boiling flow. Applied Thermal Engineering, 138, 657-667.

[14] Cole, R. (1960). A photographic study of pool boiling in the region of the critical heat flux. AIChE Journal, 6(4), 533-538.

[15] Kocamustafaogullari, G., & Ishii, M. (1983). Interfacial area and nucleation site density in boiling systems. International Journal of Heat and Mass Transfer, 26(9), 1377-1387.

[16] Basu, N., Warrier, G. R., & Dhir, V. K. (2005). Wall heat flux partitioning during subcooled flow boiling: Part 1—model development. J. Heat Transfer, 127(2), 131-140.